

Measurement of Respiratory Acoustic Signals*

Effect of Microphone Air Cavity Depth

George R. Wodicka, Ph.D.; Steve S. Kraman, M.D.;
Gerald M. Zenk, M.S.E.E.; and Hans Pasterkamp, M.D.

The use of electret microphones to measure lung sounds is widespread because of their small size, high fidelity, and low cost. Typically, an air cavity is placed between the skin surface and the microphone to convert the chest wall vibrations into a measurable sound pressure. The importance of air cavity depth on this transduction process was investigated in this study. An acoustic model of chest wall—air cavity—microphone interface was developed and the predicted effects of depth were compared with measurements performed using an arti-

ficial chest wall and lung sounds from a healthy subject. Model predictions are in general agreement with both *in vitro* and *in situ* measurements and indicate that the overall high-frequency response of the transduction diminishes with increasing cavity depth. This finding suggests that smaller cavity depths are more appropriate for detection of lung sounds over a wide band width and stresses the importance of coupler size on microphone measurements. (Chest 1994; 106:1140-44)

Key words: lung sounds, microphone, respiratory sounds

Small electret microphones are commonly used to measure lung sounds at the chest wall. Compared with contact sensors such as accelerometers that can provide a superior measurement frequency response,¹ microphones are less sensitive to extraneous skin and cable noise, are not as fragile, and are usually less expensive. These factors combined with their simplicity of use make microphones a popular choice for lung sounds measurements in a variety of research and clinical environments.

To couple chest wall vibrations into a measurable sound pressure at the microphone diaphragm, an air cavity is typically placed between the skin surface and the diaphragm. This cavity provides the interface between the vibrating chest wall and the microphone diaphragm and its response. Although many microphones have what is considered to be nearly ideal (flat) frequency response in free space, the action of the chest wall—air cavity—microphone system in concert is not ideal and is quite complex. A key determinant of the combined response is the size of the air cavity. Although the cavity diameter is often chosen to equal the microphone diameter (which is roughly 8 mm for many small electret microphones), researchers have used cavity depths ranging from a few millimeters, thereby placing the

microphone extremely close to the chest wall,² to much greater distances from the surface.^{3,4}

In this study, the effect of air cavity depth on lung sounds measurements was investigated using three approaches: (1) an acoustic model of the chest wall—air cavity—microphone interface was developed to serve as a foundation on which to understand the importance and action of the cavity; (2) an artificial chest wall with a sound generator was constructed to allow well-controlled *in vitro* acoustic measurements to be performed with various cavity depths; and (3) lung sound measurements were performed *in situ* at different cavity depths to quantify the overall effect on a moving chest wall.

METHODS

Modeling

Lumped Element Approach: The principal goal of the modeling effort was to predict the frequency-dependent effect of air cavity depth on lung sounds measurements. Since the majority of lung sound energy is confined to frequencies of <1,500 Hz, the sound wavelengths λ in the cavity as determined by the sound speed c in air (roughly 35,400 cm/s at body temperature) are longer than

$$\lambda \geq \frac{c}{f} = \frac{35,400 \text{ cm/s}}{1500 \text{ Hz}} = 23.6 \text{ cm}$$

and even longer in the chest wall as the sound speed in tissue is much greater than in air. Thus, λ is significantly greater than the thickness of the chest wall, depth of any reasonable size air cavity, and thickness of the microphone diaphragm. This dictates that the response of each of these structures to lung sounds can be described with reasonable accuracy in terms of lumped acoustic elements. To achieve predicted frequency responses accurate to within 10 percent in this type of representation, each portion of a structure represented by an acoustic element needs to be approximately $< \frac{1}{10} \lambda = 2.36 \text{ cm}$ in length. For our purposes, this results in the inherent resistance, inertance (mass), and compli-

*From the School of Electrical Engineering, Purdue University, West Lafayette, Ind (Dr. Wodicka and Mr. Zenk); The VA Medical Center, Lexington, Ky (Dr. Kraman); and the Department of Pediatrics and Child Health, University of Manitoba, Winnipeg, Canada (Dr. Pasterkamp).

Presented in preliminary form at the 18th International Conference on Lung Sounds, Lake Louise, Canada, 1993.

This study was supported in part by a grant from the Whitaker Foundation, a National Science Foundation Young Investigator Award BCS-9257488 (G.R.W.), and by the Department of Veterans Affairs.

Manuscript received September 9, 1993; revision accepted February 22, 1994.

Reprint requests: Dr. Wodicka, 1285 Electrical Engineering Bldg, Purdue University, West Lafayette, IN 47907-1285

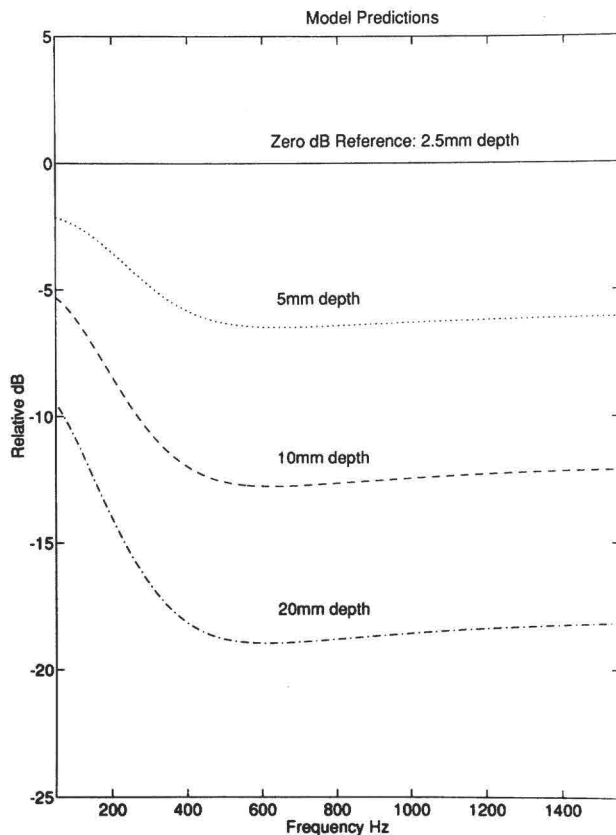


FIGURE 1. Model predictions of the effect of air cavity depth on the overall measurement response in decibel form relative to the 2.5-mm depth case.

ance of the chest wall, air cavity, and microphone diaphragm being modeled with a small number of elements with appropriate interconnections based on geometric considerations.

Simulations: Details concerning the modeling approach are found in the Appendix. Briefly, the acoustic circuit in Figure A1 was simulated on a computer using cavity depths l of 2.5, 5, 10, and 20 mm with the corresponding circuit element values for the air cavity. Both the chest wall and microphone element values were kept constant throughout the simulations. The underlying sound pressure at the chest wall p_{cw} was assumed to be uniform with respect to frequency over the 100- to 1,500-Hz range for the simulations. The choice of a uniform pressure source is appropriate in this case since only relative information concerning cavity depth was desired. After each simulation representing a particular cavity depth was performed, the sound pressure at the microphone as a function of frequency was determined relative to the smallest depth (2.5 mm) case and placed in decibel (dB) form

$$\text{dB} = 20 \log_{10} \left(\frac{p_m \text{ at a depth } l = 2.5, 5, 10, \text{ or } 20 \text{ mm}}{p_m \text{ at a depth } l = 2.5 \text{ mm}} \right)$$

and plotted in Figure 1. The reference case of $l = 2.5$ mm is depicted as a straight line independent of frequency as $20 \log_{10}(1) = 0$ dB. As l is increased, the resulting relative spectra in decibel form take on negative values as $20 \log_{10}$ of a number that is less than unity is negative. For example, a predicted relative sound pressure ratio of $1/2$ is represented as approximately -6 dB.

The model predictions indicate that with increasing cavity depth, the sound pressure at the microphone decreases in a manner that is frequency dependent. At the lowest frequencies, the pressure decreases are smallest but become more significant with

frequency up to roughly 400 Hz, where a plateau is reached. Even for the 5-mm depth case, the plateau value of approximately -6 dB is significant in terms of measurement sensitivity as it represents a 50 percent decrease in sound pressure at the microphone diaphragm for a given lung sound excitation. Larger cavity depths are predicted to decrease the overall frequency response even further, especially at the higher frequencies.

In Vitro Measurements

A simple sound source—artificial chest wall combination was constructed to test cavity depth effects under controlled conditions within a sound-proof chamber. A small bore compression driver (Peavey 22A loudspeaker) was connected directly to a 10-cm-long flanged horn with a proximal diameter of 2.2 cm and a distal diameter of 4.3 cm. A 2-cm-thick water-filled sponge that was sealed in a latex pouch was stretched across the distal opening and the pouch was in turn sealed to the circumferential border. The unit was positioned so that the outer pouch surface provided a horizontal and nearly flat surface on which to place the measurement transducers. No attempt was made to exactly match the surface impedance to that estimated for the chest wall, although it is likely to be similar to chest wall surface not overlying a rib or other bone.

Four rigid air cavities of diameter $d = 8$ mm and lengths 2.5, 5, 10, and 20 mm were tested, each with a small electret microphone (Sony ECM-155) placed flush with the distal end of the cavity and sealed. The cavities were constructed from 2-mm-thick plastic and were connected to the pouch surface with double-sided tape along the cavity circumference. Each cavity was vented with a 3-cm-long 22-gauge (inner diameter, 0.43 mm) needle to room air. For each measurement, noise with equal energy at frequencies between 200 and 1,600 Hz was applied to the driver for a

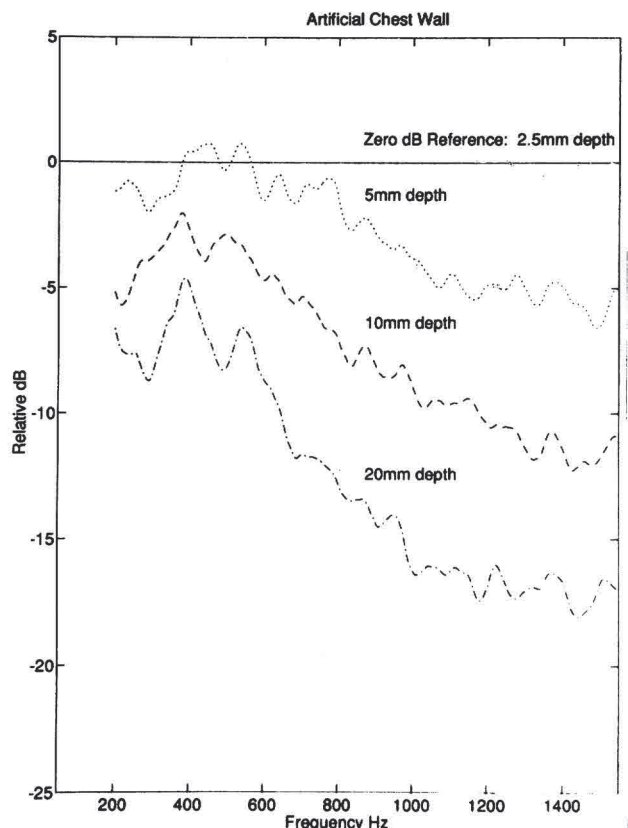


FIGURE 2. Effect of air cavity depth on measurements performed on an artificial chest wall in the same relative decibel form as in Figure 1.

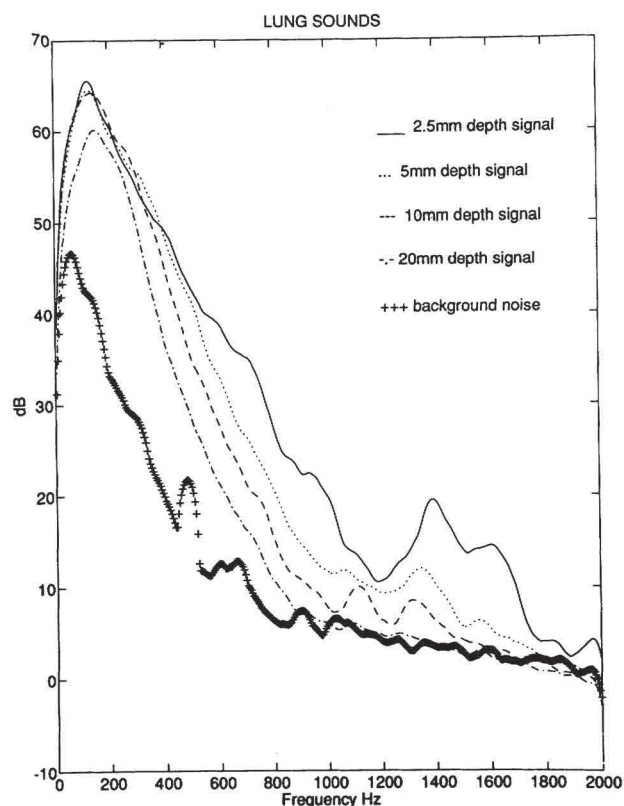


FIGURE 3. Family of curves representing air cavity depth effect on lung sounds measured at the chest wall. The ordinate scale is in arbitrary decibel units and the lowest curve represents an estimate of background (zero flow) noise.

duration of 2 s. The microphone output signal was digitized at a rate of 10,000 samples per second after bandpass filtering was performed between 100 and 2,000 Hz (four-pole Butterworth filters). The digital data were parsed into segments of 2,048 points each with 50 percent overlap between consecutive segments. Each segment was then windowed with a Hanning function and processed via a fast Fourier transform algorithm. The resulting power spectra were averaged in the frequency domain to form a single spectral estimate for a particular cavity depth. Finally, to be consistent with the presentation for the model predictions, the spectra across depths were plotted in the same decibel form relative to the 2.5-mm depth case.

The results of this measurement and processing procedure are summarized in Figure 2 noting that both the abscissa and ordinate scales are identical to those in Figure 1. The same overall trend of decreasing sensitivity at higher frequencies with increasing cavity depth is observed as was predicted by the model, yet the relative responses are considerably more complex. The differences between responses at each cavity depth with frequency trend as predicted, but do so over a larger frequency range and thus do not appear to reach a plateau until at least 1,000 Hz. At the highest measured frequency of 1,600 Hz, the measurements are extremely close to the predictions. However, at lower frequencies, the deviations between theory and experiment are greatest, with the 5-mm depth yielding equal to or greater sensitivity as compared with the 2.5-mm depth over a small frequency band.

In Situ Measurements

The study protocol was approved by the Purdue University Committee on the Use of Human Subjects, and one of the inves-

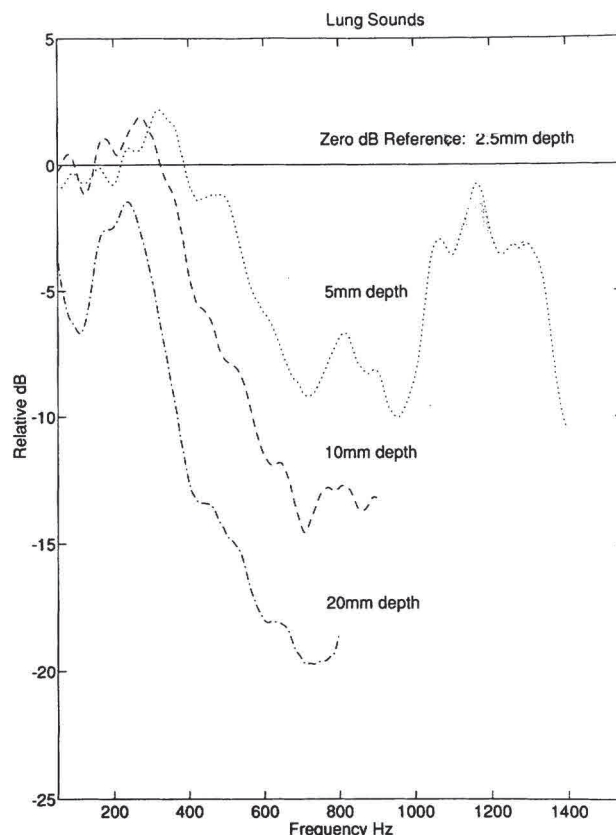


FIGURE 4. Effect of air cavity depth on lung sounds measurements in the same relative decibel form as in Figures 1 and 2.

tigators (S.S.K.) served as the subject after providing informed consent. The subject was a healthy nonsmoking man without a history of chronic respiratory disease or a respiratory tract infection for 1 month prior to the study. The anatomic point of maximum lung sound intensity on the right anterior chest was identified by auscultation prior to the investigation and this site was used for the entire procedure.

The subject sat in a sound-proof chamber with nose clips on and breathed through a calibrated pneumotachograph. A target flow range of 2 L/s was set and the subject received feedback concerning his flow rate via an oscilloscope. As was the case for the *in vitro* measurements, the air cavity-microphone arrangements were connected to the chest wall with double-sided tape around the circumference. The lung sounds were amplified, filtered, and digitized as previously described. During the sampling process, digital-to-analog playback of the sounds to the investigators ensured artifact-free recording over at least four complete respiratory cycles at each cavity depth. The digital data that corresponded to inspiratory flows between 1.5 and 2.5 L/s were selected and analyzed in an identical fashion to the *in vitro* measurements. The resulting average power spectra for an individual cavity depth are shown in arbitrary decibel units in Figure 3. The spectra for the background noise were estimated from samples within a nearly zero flow rate of 0.0 to 0.1 L/s. These spectral plots are presented in relative decibel form in Figure 4 to facilitate comparisons with Figures 1 and 2.

As depicted in Figure 3, the effective bandwidth of the lung sounds measurements decreased with increasing cavity depth. The frequency at which the lung sounds spectral estimate reached that of the background noise (which was essentially identical regardless of depth) ranged from approximately 1,700 Hz for the

2.5-mm case to 800 Hz for the 20-mm case. This finding supports the prediction that smaller cavity depth yields improved overall high-frequency response. It also confirms recent findings of lung sounds energy extending well beyond previously assumed high-frequency limits of roughly 1,000 Hz. Given this depth-dependent bandwidth, the curves in Figure 4 are plotted only over regions where the lung sounds energy was above that of background noise.

As compared with Figures 1 and 2 representing the model predictions and the *in vitro* measurements, respectively, the relative lung sounds spectra also exhibit many of the general trends that were predicted yet extend many of the complexities noted in the previous measurements. The differences in the sensitivity to lung sounds at low frequencies were quite small except for the largest cavity depth. These differences grow rapidly with frequency from about 200 to 600 Hz in a similar fashion to the model prediction reaching -6 dB amplitude reduction points at roughly 320, 460, and 630 Hz for the 5-, 10-, and 20-mm depths. Yet instead of reaching a plateau at higher frequencies, the responses had multiple peaks that may represent heterogeneities in both the lung sound source and the chest wall. However, it remains clear that the smallest cavity ensures the greatest sensitivity of the response to higher-frequency lung sounds.

DISCUSSION

As the field of respiratory acoustics matures, the need to understand fundamental transduction issues increases as more measurements using different sensors under varied conditions are performed. Although the scope of this study was rather narrow—investigation of a specific coupling parameter (cavity depth) for a particular type of sensor (electret microphone)—the results indicate that even for a given sensor, the overall frequency response depends strongly on the coupling arrangement. In this case, smaller cavity depths yield improved response at higher frequencies. This observation may explain why lung sounds measured with a stethoscope have been characterized as having little appreciable energy above 1,000 Hz.

The lumped-parameter model served as a mechanism to understand the importance of cavity depth on the measurements. Although our approach included a number of assumptions, the observed magnitude and frequency dependence of the cavity effects were predicted reasonably well. The model predicts that a long cavity with a large compliance C_c does not sustain as large a pressure at the microphone p_m for a given chest wall movement U_{cw} relative to a smaller cavity. As the measurements moved from the bench top to the moving chest wall, quantitative differences between measurements and predictions grew. These differences were likely to be due to a number of factors, including deviations of the artificial and subject's chest wall impedance values from those used in the model, heterogeneity of the chest wall (including bone) that was not represented, as well as errors inherent to the spectral estimation procedure.

This depth dependence does not necessarily apply when a diaphragm is placed on the chest wall surface

to couple vibrations to a microphone as in many electronic stethoscopes.⁵ In this case, the properties of the diaphragm and its interaction with both the chest wall and the air cavity dictate the overall response which can be much more complex given the additional design parameters. As a number of investigators continue to employ electronic stethoscopes in the measurement of lung sounds, understanding their properties better in terms of coupling arrangements would be useful to allow comparisons to be made with other types of sensors and couplers. Also, other geometric factors such as cavity diameter and volume for air-coupled measurements need to be quantified.

APPENDIX

Acoustic Circuit

Figure A1 depicts the acoustic circuit that was used to represent the chest wall—air cavity—microphone interface. In the circuit, sound pressure p in N/m^2 is the across element variable analogous to electrical voltage, and volume velocity U in m^3/s is the through element variable analogous to electrical current. Acoustic impedance Z is defined as the ratio of sound pressure to volume velocity

$$Z = \frac{p}{U}$$

in units of Ns/m^5 , with Z_{cw} , Z_c , and Z_m representing the chest wall, cavity, and microphone impedance, respectively. A key determination is the effect of changing cavity depth and thus Z_c on the relationship between sound pressure measured at the microphone p_m and underlying vibration of the chest wall U_{cw} due to lung sound excitation at the chest wall p_{cw} .

Chest Wall Impedance

The acoustic impedance of the chest wall has been measured by a number of investigators using various experimental techniques.⁶ At frequencies below 1,500 Hz, the impedance is represented well by a series acoustic resistance-compliance-inertance interconnection with a highly damped resonance at just above 200 Hz. Below resonance, the compliance of the chest wall dominates the overall Z_{cw} while above reso-

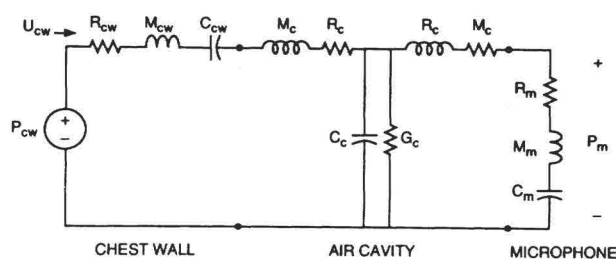


FIGURE A1. Acoustic circuit model in element form. Both the chest wall and the microphone diaphragm are represented by series R-M-C interconnections that are connected via an air cavity modeled by a T equivalent circuit.

nance, the inertance is most significant. Assuming a cavity diameter $d=8$ mm, estimated element values are as follows:

acoustic resistance	$R_{cw}=8 \times 10^8$	Ns/m ⁵
acoustic compliance	$C_{cw}=2.5 \times 10^{-12}$	m ⁵ /N
acoustic inertance	$M_{cw}=2 \times 10^5$	kg/m ⁴

which in a series interconnection has a resonance frequency

$$f_o = \frac{1}{2\pi} (C_{cw} M_{cw})^{-1/2} = 225 \text{ Hz}$$

Microphone Impedance

The acoustic impedance of a microphone diaphragm can also be accurately modeled as a series resistance-compliance-inertance interconnection.⁷ Since in the experimental parts of this study an electret microphone (Sony ECM-155) was used, its particular characteristics were derived from the manufacturer's specifications, noting that they are quite similar to a number of microphones from other manufacturers. The element values are as follows:

$R_m=1 \times 10^8$	Ns/m ⁵
$C_m=3.6 \times 10^{-14}$	m ⁵ /N
$M_m=3.3 \times 10^2$	kg/m ⁴

As compared with the chest wall, the microphone diaphragm is much less massive and compliant and thus has a considerably higher resonance frequency.

Air Cavity Impedance

The air cavity was represented as a rigid cylinder of diameter $d=8$ mm that was filled with air in contact with the chest wall at one end and the microphone diaphragm at the other. To represent the cylindrical cavity in terms of acoustic circuit elements, a T configuration as shown in the middle of Figure A1 was used. Here C_c represents the air compliance of the cavity with associated thermal conductive losses G_c , and M_c represents the air inertance with associated viscous resistive loss R_c . The total inertance and viscous loss is split into two components each to provide a more accurate spatial description of the cavity response. Values of the circuit elements are determined from acoustic theory⁸ and can be written for this case in terms of the depth l (in m) of the cavity

$$C_c = \frac{Al}{\rho c^2} = 3.5 \times 10^{-10} l \quad \text{m}^5/\text{N}$$

$$M_c = \frac{\rho l}{2A} = 11.4 \times 10^3 l \quad \text{kg/m}^4$$

$$R_c = \frac{S}{2A^2} (\pi f \rho \mu)^{1/2} l = 1.3 \times 10^6 l \quad \text{Ns/m}$$

$$G_c = \frac{0.4S}{\rho c^2} \left(\frac{\pi f \gamma}{\rho \alpha} \right)^{1/2} l = 1.77 \times 10^{-8} l \quad \text{m/Ns}$$

where

$$A = \text{cross sectional area} = \frac{\pi d^2}{4} = 5 \times 10^{-5} \quad \text{m}^2$$

$$\rho = \text{density of air} = 1.14 \quad \text{kg/m}^3$$

$$S = \text{circumference} = \pi d = 2.5 \times 10^{-2} \quad \text{m}$$

$$\mu = \text{viscosity coefficient} = 1.86 \times 10^{-5} \quad \text{Ns/m}^2$$

$$\gamma = \text{coefficient of heat conduction} = 0.55 \times 10^{-1} \quad \text{cal/sm}^\circ\text{C}$$

$$\alpha = \text{specific heat of air at constant p} = 0.24 \times 10^{-3} \quad \text{cal/kg}^\circ\text{C}$$

Letting $l=2.5$ mm $= 2.5 \times 10^{-3}$ m to compare cavity element values to those for the chest wall and microphone yields $C_c=8.75 \times 10^{-13}$ which is roughly half C_{cw} and $M_c=2.85 \times 10^1$ which is smaller than M_m . In other words, the acoustic compliance of a very small air cavity is near to that exhibited by the chest wall itself but the air inertance is negligible relative to that of the chest wall and microphone. Estimated values of both R_c and G_c also yield small overall effects. Thus, the most important contribution of the air cavity to the frequency response of the system is to provide an acoustic compliance that converts chest wall vibrational motion into a sound pressure that is detected at the microphone diaphragm.

It should be noted that in many coupler designs, the cavity is vented to atmospheric pressure via a small needle or conduit to avoid significant diaphragm displacement due to static pressure buildup or release. In the circuit model of the cavity, such a venting conduit would be incorporated as an impedance essentially in parallel to Z_c yet terminating in a (grounded) zero pressure point. Typically the conduit diameter is chosen small enough (eg, <0.5 mm) and the length long enough (eg, >20 mm) so that this parallel impedance is extremely large as compared with the air cavity impedance at acoustic frequencies. Thus, the overall effect of venting on lung sounds measurements is very small while it provides an assurance of zero static pressure within the cavity.

REFERENCES

- 1 Pasterkamp H, Kraman SS, DeFrain PD, Wodicka GR. Measurement of respiratory acoustical signals: comparison of sensors. *Chest* 1993; 104:1518-25
- 2 Kraman SS. Effects of lung volume and air flow on the frequency spectrum of vesicular lung sounds. *Respir Physiol* 1986; 66:1-9
- 3 Charbonneau G, Racineux JL, Sudraud M, Tuchais E. An accurate recording system and its use in breath sounds spectral analysis. *J Appl Physiol* 1983; 55:1120-27
- 4 Druzgalski CK, Donnerberg RL, Campbell RM. Techniques of recording respiratory sounds. *J Clin Eng* 1980; 5:321-29
- 5 Anderson K, Aitken S, Carter R, MacLeod JE, Moran F. Variation of breath sound and airway caliber induced by histamine challenge. *Am Rev Respir Dis* 1990; 141:1147-50
- 6 Verburg J, van Vollenhoven E. Phonocardiography: physical and technical aspects and issues. In: Rolfe P, ed. *Noninvasive physiological measurements*. London: Academic Press, 1979; 213-59
- 7 Beranek LL. *Acoustics*. New York: American Institute of Physics, 1988
- 8 Flanagan JL. *Speech analysis: synthesis and perception*. Berlin: Springer-Verlag, 1983